

Concise Geometric Description as a Bridge: Unleashing the Potential of LLM for Plane Geometry Problem Solving

Jingyun Wang¹, Dian Li[‡], Xiaohan Wang, Gang Liu, Jiahong Yan, Guoliang Kang^{1‡}

¹Beihang University
 {wangjingyun0730, kgl.prml}@gmail.com

Abstract

Plane Geometry Problem Solving (PGPS) is a multimodal reasoning task that aims to solve a plane geometric problem based on a geometric diagram and problem textual descriptions. Although Large Language Models (LLMs) possess strong reasoning skills, their direct application to PGPS is hindered by their inability to process visual diagrams. Existing works typically fine-tune Multimodal LLMs (MLLMs) end-to-end on large-scale PGPS data to enhance visual understanding and reasoning simultaneously. However, such joint optimization may compromise base LLMs' inherent reasoning capability. In this work, we observe that LLM itself is potentially a powerful PGPS solver when appropriately formulating visual information as textual descriptions. We propose to train a MLLM Interpreter to generate geometric descriptions for the visual diagram, and an off-the-shelf LLM is utilized to perform reasoning. Specifically, we choose Conditional Declaration Language (CDL) as the geometric description as its conciseness eases the MLLM Interpreter training. The MLLM Interpreter is fine-tuned via CoT (Chain-of-Thought)-augmented SFT followed by GRPO to generate CDL. Instead of using a conventional solution-based reward that compares the reasoning result with the ground-truth answer, we design CDL matching rewards to facilitate more effective GRPO training, which provides more direct and denser guidance for CDL generation. To support training, we construct a new dataset, Formalgeo7k-Rec-CoT, by manually reviewing Formalgeo7k v2 and incorporating CoT annotations. Extensive experiments on Formalgeo7k-Rec-CoT, Unigeo, and Math-Vista show our method (finetuned on only 5.5k data) performs favorably against leading open-source and closed-source MLLMs.

Table 1. **LLMs are potentially powerful PGPS solvers.** “Visual” refers to MLLMs reasoning with visual inputs, while “Caption” and “GT CDL” refer to MLLMs and LLM reasoning with captions generated by Gemini-2.5 Pro or ground-truth CDL annotations, but without access to visual modality. Results demonstrate that, converting visual information into appropriate textual descriptions, LLM itself is a potentially powerful PGPS solver.

Models	Type	Visual	Caption	GT CDL
Claude-Opus-4.1	MLLM	69.1	76.8	84.2
Gemini2.5-Pro		81.8	81.1	84.3
Qwen3 30B	LLM	-	82.1	88.4

1. Introduction

Plane Geometry Problem Solving (PGPS) is a multimodal task that requires solving a problem based on a geometric diagram and its accompanying textual description. This task presents a significant challenge, as it demands both complex visual perception and rigorous logical reasoning capabilities. Though Large Language Models (LLMs) possess powerful reasoning skills, their direct application to PGPS (Fig. 1(b)) is severely constrained without access to the visual modality.

Conventional PGPS methods [4, 8, 21, 22, 38, 41, 42] turn to fine-tuning Multi-modal Large Language Models [1, 17, 28] (MLLMs) on large-scale datasets to simultaneously enhance their visual understanding and reasoning capabilities. Despite the progress achieved, such a joint optimization paradigm remains unsatisfactory: On one hand, in Figure 1(a), MLLMs still suffer from significant visual perception errors (e.g., misidentifying $\angle ACE$ as 33° instead of $\angle ECB$). On the other hand, end-to-end training may inevitably compromise the inherent reasoning skills of the base LLMs. Moreover, we observe that (Table 1) **LLMs are potentially powerful PGPS solvers when formulating visual information as textual descriptions.** The preceding analysis motivates us to explore a new paradigm:

[†]Project leader.

[‡]Corresponding authors.

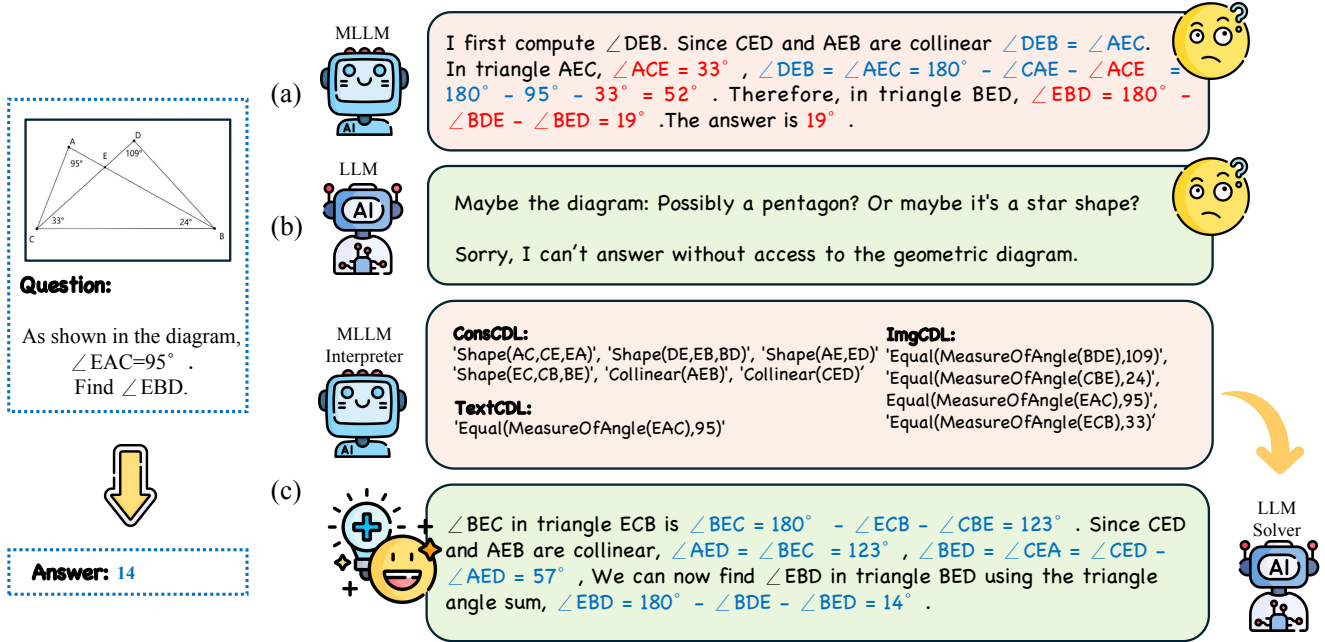


Figure 1. (a) **MLLMs.** Though MLLMs can directly perform PGPS, they still suffer from heavy visual perception errors or logical reasoning errors. (b) **LLMs.** LLMs are not capable of PGPS without access to geometric diagrams. (c) **Ours.** We employ a MLLM interpreter to convert geometric diagrams into a concise CDL description upon which an LLM solver performs reasoning.

converting geometric inputs into textual descriptions to unleash the reasoning power of LLMs for PGPS.

In this paper, we propose a novel paradigm for PGPS. As illustrated in Figure 1(c), we train a MLLM Interpreter to convert geometric inputs into concise geometric descriptions, *i.e.*, Conditional Declaration Language (CDL) [40] (as shown in pink box of Fig. 1(c)). The MLLM Interpreter is initialized with an open-source MLLM and fine-tuned via a two-stage pipeline: a CoT-augmented Supervised Fine-Tuning (SFT) stage followed by a Group Relative Policy Optimization [27] (GRPO) stage. Instead of using a conventional solution-based reward that compares the reasoning result with the ground-truth answer, we design CDL matching rewards to facilitate more effective GRPO training, which provides more direct and denser guidance for CDL generation. Specifically, we greedily match generated CDL and the ground-truth CDL piece-by-piece and design parsing rules to enable accurate matching. The CDL rewards consist of the recall and precision of the matching results. Finally, with the generated geometric descriptions as the bridge, an off-the-shelf LLM Solver is utilized to perform reasoning. Our practice reveals two technical insights 1) Concise geometric descriptions ease the MLLM Interpreter’s learning by narrowing the search space. 2) Compared to solution-based rewards, our CDL matching rewards design is more effective in GRPO as it provides more direct and denser guidance for CDL generation.

To support the training, we construct a new dataset,

Formalgeo7k-Rec-CoT. We conduct a rigorous manual review on Formalgeo7k v2 [42] to fix annotation errors and parse CDL annotations to generate Chain-of-Thoughts (CoTs). We conduct extensive experiments on various PGPS benchmarks, including Formalgeo-Rec-CoT, Uni-geo [4], and the geometric set of MathVista [18]. Our method is compared with various leading open-source and closed-source MLLMs. The results demonstrate that our method consistently outperforms all open-source MLLMs and obtains comparable performance to leading closed-source MLLMs.

In a nutshell, our contributions are summarized as:

- We observe LLM itself is a powerful PGPS solver when provided geometric information appropriately. Thus, we propose a new paradigm that trains a MLLM Interpreter to generate geometric descriptions and utilizes an off-the-shelf LLM for reasoning.
- We train the MLLM Interpreter with CoT-augmented SFT and GRPO with specifically designed CDL matching rewards. Our practice reveals two technical insights 1) Concise geometric descriptions ease the MLLM Interpreter’s learning by narrowing the search space. 2) CDL matching rewards are more effective in GRPO as they provide more direct and denser guidance for CDL generation than solution-based rewards.
- We propose Formalgeo7k-Rec-CoT by conducting a rigorous manual review on Formalgeo7k v2 to fix annotation errors and parsing annotations to generate

CoTs to support CDL generation training.

- With only 5.5k training data, our method performs favorably against leading open-source and closed-source MLLMs on PGPS benchmarks.

2. Related Work

Multi-modal Large Language Model (MLLM). Building upon breakthroughs in Large Language Models (LLMs) [2, 9, 13, 19, 29, 30, 33, 34] and Vision Foundation Models (VFM) [14, 15, 23, 37], Multi-modal Large Language Models (MLLMs) [1, 6, 12, 17, 20, 28] emerge as a powerful paradigm, which integrates visual perception with the reasoning capabilities of LLMs. Through massive-scale pre-training data and advanced training strategies [24, 26, 27, 36], MLLMs make great progress in a wide range of multi-modal tasks, including visual question answering and image captioning. However, their performance remains unsatisfactory in domains requiring rigorous reasoning (*e.g.*, Plane Geometry Problem Solving). A key limitation is that the inherent reasoning ability of their base LLMs might be compromised as MLLMs jointly optimize their visual perception and linguistic reasoning capabilities.

Plane Geometry Problem Solving (PGPS). Most methods for Plane Geometry Problem Solving (PGPS) [3, 5, 7, 8, 11, 16, 31, 32, 38, 39] fine-tune Multi-modal Large Language Models (MLLMs) in an end-to-end manner on large-scale training data. For example, PGPSNet [38] constructs PGPS9K and G-LLaVA constructs Geo170K for training. However, such end-to-end fine-tuning inevitably compromises the inherent reasoning capabilities of the base Large Language Models (LLMs). Another line of work, including GF Reasoner [35] and LVDA [10], explores converting diagrams into textual descriptions for geometric solvers. Despite the progress, these methods face significant limitations: From one aspect, their reliance on general textual descriptions introduces substantial redundancy in the search space, which harms both description generation and solving performance. From the other aspect, the unstructured nature of general textual descriptions makes matching rewards in GRPO infeasible, forcing reliance on an extra solver that provides an extremely sparse reward signal. Beyond previous works, our method transforms geometric inputs into concise geometric descriptions, effectively addressing these limitations and fully leveraging the reasoning power of LLMs for PGPS.

3. Method

Overview In this work, we propose a new paradigm that firstly trains a MLLM Interpreter to generate geometric descriptions for the visual diagram, and then employs an off-the-shelf LLM to perform reasoning. The overall framework is illustrated in Fig. 2. The MLLM Interpreter

(Sec. 3.1) is trained with a two-stage pipeline to convert geometric diagrams into textual descriptions.

3.1. MLLM Interpreter

3.1.1. Conditional Declaration Language (CDL)

Definition of CDL. We choose Conditional Declaration Language (CDL) [40] as the geometric description. CDL consists of construction statements (ConsCDL) and condition statements (ImgCDL and TextCDL): ConsCDL defines the fundamental structure of the diagram, *e.g.*, basic shapes, collinear, and cocircular. ImgCDL and TextCDL specify the geometric and algebraic relations derived from the diagram (ImgCDL) and the problem text (TextCDL), such as the length of line segment or parallel relationships. Based on topological mapping, CDL offers a unified and rigorous framework for representing plane geometric inputs.

Conciseness of CDL. Compared with general textual descriptions, CDL offers a more structured and concise representation (the proof for CDL’s conciseness can be found in the appendix). Such conciseness inherently narrows the search space and we empirically find that this conciseness benefits the training of MLLM Interpreter (see Sec. 4.3 for more details).

3.1.2. Formalgeo7k-Rec-CoT

Formalgeo7k v2 [42] is a dataset containing multiple question-answer pairs equipped with corresponding diagrams and CDL annotations. Based on Formalgeo7k v2, we construct Formalgeo7k-Rec-CoT for training.

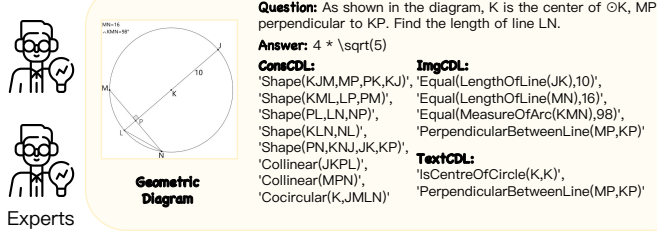
Manual Review. We identify data quality issues in Formalgeo7k v2, including diagram-question mismatching and incorrect CDL annotations. To improve the quality of data, we conduct a rigorous manual review. The review process is completed by four qualified annotators. To ensure objectiveness and consistency, each piece of data is independently reviewed by two annotators. A modification is applied when a consensus is reached by both annotators; any discrepancy will be adjudicated by the third annotator.

Chain-of-Thought (CoT) Incorporation. To guide the MLLM Interpreter to perform step-by-step reasoning for CDL generation, we incorporate Chain-of-Thought (CoT) into Formalgeo7k-Rec-CoT. The data is structured with special tokens to separate the reasoning process from the CDL output, following the format: <think> CoT here </think> <cdl> CDL here </cdl>. To automatically generate CoT sequences, we develop a Python parser that extracts and processes geometric information from CDL annotations. As shown in Fig. 2(a), the parser translates the symbolic relations into natural language reasoning steps, creating training pairs for the Supervised Fine-Tuning (SFT) stage.

3.1.3. Stage 1: SFT with CoT-Augmented Data

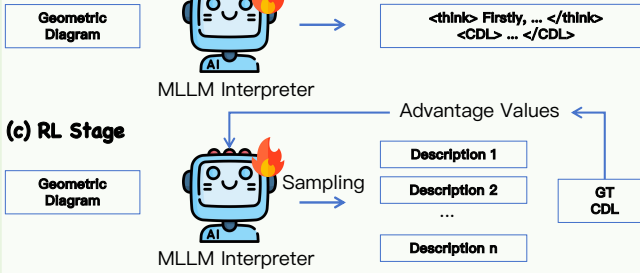
We perform supervised fine-tuning (SFT) on the MLLM Interpreter (*e.g.*, Qwen 2.5-VL and Qwen 3-VL series) us-

(a) Data Construction

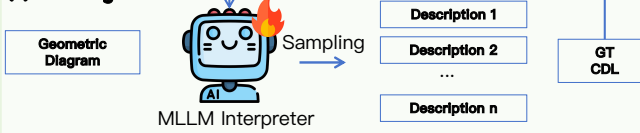


Cot: Firstly, looking into the diagram, I see **6 points**, they are L, P, J, M, K, N. And I see **1 circle**, the centroid of it is K. Points JMLN lie on Circle K, they are **cocircular points**, so we get Cocircular(K, JMLN). Among all points, I observe their **connection relationship**. I see Point N and Point P are connected by line segment NP. I see Point M and Point L are connected by Arc ML on Circle K. Furthermore, I observe some **collinear relationship**. Points J, K, P, L lie on a single straight line, so they are collinear and we get Collinear(JKPL) I then look into the shapes in this geometric diagram. Now I identify some **closed shapes**. I identify a closed shape formed by arc JM on circle K, line segment MP, line segment PK, line segment KJ, represented as Shape(KJM,MP,PK,KJ)

(b) SFT Stage



(c) RL Stage



(d) Solving

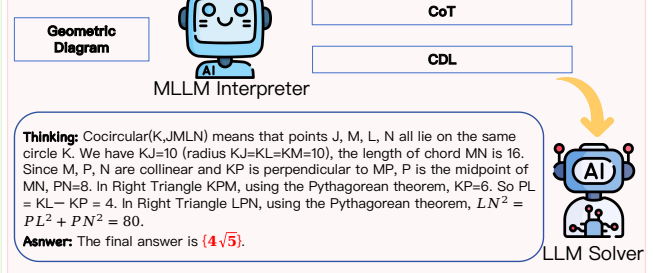


Figure 2. Method Overview. (a) **Data Construction**. We construct **Formalgeo7k-Rec-CoT** by manual reviewing Formalgeo7k v2 and incorporating the Chain-of-Thought (CoT). We design a two-stage pipeline to train MLLM Interpreter, including a (b) **CoT-Augmented SFT Stage** and a (c) **GRPO Stage with CDL Matching Rewards**. Based on the generated CDL, an (d) **LLM Solver** directly performs reasoning and derives final solutions.

ing the CoT-augmented training data in Formalgeo7k-Rec-CoT. The training objective is to minimize the negative log-likelihood of the reasoning steps and final textual description output:

$$\min_{\theta} \mathbb{E}_{(x, r, y) \sim \mathcal{D}} [-\log \pi_{\theta}(r, y|x)] \quad (1)$$

where \mathcal{D} denotes our training data containing textual description annotations paired with reasoning steps, x denotes the input, r denotes the reasoning process, y denotes the final textual description output, and π_{θ} is the probability distribution of the MLLM Interpreter parameterized by θ . The SFT stage serves as a warm-up phase, equipping the MLLM Interpreter with step-by-step reasoning capability for CDL generation. However, we observe that SFT alone yields suboptimal performance. We hypothesize that the standard next-token prediction objective of SFT may inadequately capture the precise logical constraints. To address the limitation, we explore Group Relative Policy Optimization (GRPO) with CDL matching rewards.

3.1.4. Stage 2: GRPO with CDL Matching Rewards

Group Relative Policy Optimization (GRPO). During the Reinforcement Learning (RL) stage, we adopt the Group Relative Policy Optimization (GRPO) algorithm [27], which optimizes the policy by directly sampling and comparing groups of candidate responses. Given an input x , GRPO samples n candidate responses $\{(r_1, y_1), (r_2, y_2), \dots, (r_n, y_n)\}$ from the old policy π_{old}

and evaluates each response by a reward function, producing a set of scores $\{s_1, s_2, \dots, s_n\}$. To determine the relative quality of these responses, GRPO normalizes the scores by computing their mean and standard deviation, and then calculates the advantage for each candidate:

$$A_i = \frac{s_i - \text{mean}(s_1, s_2, \dots, s_n)}{\text{std}(s_1, s_2, \dots, s_n)}, \quad (2)$$

where A_i quantifies the advantage of the response (r_i, y_i) relative to other sampled responses. The policy π_{θ} is updated by maximizing the following objective function, which promotes responses with higher advantages while maintaining stability via a KL divergence penalty \mathbb{D}_{KL} :

$$\mathcal{J}(\theta) = \frac{1}{N} \sum_{i=1}^n \{\min[o_1 \cdot A_i, o_2 \cdot A_i]\} - \beta \mathbb{D}_{KL}[\pi_{\theta} || \pi_{ref}], \quad (3)$$

$$o_1 = \frac{\pi_{\theta}((r_i, y_i)|x)}{\pi_{\theta_{old}}((r_i, y_i)|x)}, \quad (4)$$

$$o_2 = \text{clip}\left(\frac{\pi_{\theta}((r_i, y_i)|x)}{\pi_{\theta_{old}}((r_i, y_i)|x)}, 1 + \epsilon, 1 - \epsilon\right), \quad (5)$$

where π_{ref} denote the policy of reference model and ϵ, β are constants.

Rewards. We design specialized rewards in this stage, including CDL matching rewards S_C , S_I , S_T , and Format

Reward S_f . Conventional methods rely on an external LLM solver to derive a solution-based reward. However, such a solution-based reward is a holistic measure that evaluates the entire set of CDL pieces. This signal provides sparse guidance, especially when training data is limited and the sampling space is constrained, leading to ineffective optimization. Instead, we employ CDL matching rewards to provide direct and denser supervision for the generated descriptions.

(1) CDL Matching Rewards. We design matching rewards S_C, S_I, S_T for ConsCDL, ImgCDL, and TextCDL, respectively. With matching rewards, we aim to encourage the completeness of CDL generation (*i.e.*, high recall) and punish inaccuracy and repetitions (*i.e.*, high precision). Thus, we choose to evaluate the recall and precision of CDL generation results by performing greedy matching.

We take the matching reward for ConsCDL S_C as an example. We implement a Python script to judge the matching of ConsCDL, *e.g.*, two pieces that refer to the same geometric shape are considered a matched pair. Formally, let $G = \{g_1, g_2, \dots, g_m\}$ be the ground truth set, while $P = \{p_1, p_2, \dots, p_n\}$ be the predicted set. The algorithm iterates through each predicted item $p \in P$, and searches for the first item in the current ground truth set $g \in G$ that exactly matches p . Once finding a match, the corresponding ground truth item g is removed from G . This process continues until all items in the predicted set P are evaluated or the ground truth set becomes empty.

We denote the remaining set of unmatched ground truth items after this procedure as G' , so the number of successfully matched pairs is then $M = m - |G'|$. We measure the *recall* score R_{ConsCDL} to encourage completeness of ConsCDL generation, and measure the *precision* score A_{ConsCDL} to penalize inaccurate or repeated pieces. The final reward S_C is defined as the average of the precision score and the recall score

$$R_{\text{ConsCDL}} = \frac{M}{m}, P_{\text{ConsCDL}} = \frac{M}{n}, \quad (6)$$

$$S_C = \frac{R_{\text{ConsCDL}} + P_{\text{ConsCDL}}}{2}. \quad (7)$$

Matching reward for ImgCDL S_I and TextCDL S_T are calculated in the same way as that for S_C .

(2) Format Reward S_f We also design a format reward S_f to evaluate whether the model’s output strictly follows the format that requires the model to output special tags (*e.g.*, `<think> ... </think> <cdl> ... </cdl>`). The reward is set to 1 if the output complies with the formatting rules; otherwise, the reward is 0.

The overall reward is calculated as

$$S = \alpha S_f + \gamma S_C + (1 - \alpha - \gamma)(S_I + S_T), \quad (8)$$

where α and γ are constants set to 0.1 and 0.5.

3.2. LLM Solver with Generated CDL

We adopt an off-the-shelf LLM (*e.g.*, Qwen3 30B [34]) to finalize the PGPS task. Specifically, LLM solver utilizes the generated CDL from the MLLM Interpreter without the CoT as input. Based on the generated CDL, the LLM Solver performs reasoning and derives the final answer.

4. Experiment

4.1. Setup

Base Model. We conduct experiments with Qwen 2.5-VL [1] series and Qwen 3-VL series as the MLLM Interpreter. For the LLM solver, we adopt Qwen3 30B [34] for its strong logical reasoning capability.

Training Dataset. We utilize the constructed Formalgeo7k-Rec-CoT as our training dataset. Originally, Formalgeo7k v2 [42] contains 7,000 geometric question-answer pairs, each equipped with a diagram and corresponding CDL annotation. We construct Formalgeo7k-Rec-CoT by conducting a rigorous manual review on Formalgeo7k v2 and incorporating Chain-of-Thoughts (CoTs). Then, we randomly divide Formalgeo7k-Rec-CoT into training and validation sets with a ratio of 0.8 and 0.2, resulting in 5,550 pairs for training and 1,390 pairs for validation.

Implementation details. For the MLLM Interpreter, the SFT stage runs for 3 epochs with batch size 8 and learning rate $1e - 5$. The RL stage lasts for 15 epochs with batch size 128, learning rate $1e - 6$, and a rollout number $N = 8$. The LLM solver is always kept frozen.

Evaluation Benchmarks. Firstly, we evaluate the CDL generation performance of the MLLM Interpreter on the validation set of Formalgeo7k-Rec-CoT. Besides, to evaluate the plane geometric problem-solving performance of our method, we utilize both in-domain benchmark Formalgeo7k-Rec-CoT and out-of-domain benchmarks, including Unigeo [4] and the geometric set of MathVista [18]. All evaluations are open-ended: we extract the final answer from the LLM solver’s response and compare it with the ground truth to judge correctness.

4.2. Quantitative Results

4.2.1. CDL Generation

Baseline. We compare the CDL Generation against two previous models, Fgeo-Parser [42] and Diagram Formalizer [41], on the validation set of Formalgeo7k-Rec-CoT. Fgeo-Parser [42] employs two separate parsers: a diagram parser based on BLIP [15] to convert geometric diagrams into ConsCDL and imgCDL, and a text parser based on T5 [25] to transform problem textural description into textCDL. Both parsers are trained on an augmented version of the Formalgeo7k v2 training set with 14,700 samples. Diagram Formalizer [41] is trained on large-scale

Table 2. **Comparison of CDL Generation performance on Formalgeo-Rec-CoT.** Fgeo-Parser [42] employs a diagram parser (denoted as “(Diag.)”) to convert geometric diagrams into ConsCDL and ImgCDL, and a text parser (denoted as “(Text)”) to transform problem textural description into textCDL. Diagram Formalizer [41] is designed solely for parsing geometric diagrams into ConsCDL and ImgCDL. Our proposed MLLM Interpreter can process both diagrams and text with a unified model and exhibits strong overall performance.

Methods	Pub. & Year	Training Data	TextCDL		ImgCDL		ConsCDL	
			Recall	Precision	Recall	Precision	Recall	Precision
FgeoParser (Diag.) [42]	Symmetry’24	14.7k	-	-	77.5	-	87.0	-
FgeoParser (Text) [42]			96.5	-	-	-	-	-
Diagram Formalizer [41]	ICASSP’25	1M	-		92.9	-	90.3	-
Qwen2.5-VL 3B (SFT)	Ours	5.5k	94.7	94.7	94.7	92.2	62.3	58.7
Qwen2.5-VL 3B (RL)			98.9	98.9	96.5	96.9	87.1	87.6
Qwen2.5-VL 7B (SFT)			96.5	96.6	95.1	93.5	70.0	68.3
Qwen2.5-VL 7B (RL)			99.1	99.1	97.0	96.9	92.7	92.1
Qwen3-VL 4B (SFT)	Ours	5.5k	97.1	97.1	96.4	95.1	80.9	79.4
Qwen3-VL 4B (RL)			99.1	99.1	97.2	97.2	95.4	95.1
Qwen3-VL 8B (SFT)			97.2	97.2	96.0	95.0	80.9	79.6
Qwen3-VL 8B (RL)			99.2	99.3	97.0	96.9	95.9	95.8

Table 3. **Effect of CoT in CDL generation.** We perform the experiments on Qwen2.5-VL 7B. Results show that incorporating CoT of ConsCDL into the training data boosts both CDL generation performance and solving accuracy. CoTs of ImgCDL and TextCDL introduce extra tokens but degrade the performance. Considering both training cost and performance, we only utilize CoT of ConsCDL.

ConsCDL	ImgCDL	TextCDL	TextCDL		ImgCDL		ConsCDL		Formalgeo
			Recall	Precision	Recall	Precision	Recall	Precision	
			99.1	98.4	97.0	96.9	81.7	81.5	76.3
✓			99.1	99.1	97.0	96.9	92.7	92.1	83.2
✓	✓		98.5	98.4	97.0	97.1	92.4	92.0	82.8
✓		✓	99.1	99.1	96.9	96.9	92.0	91.7	81.7

datasets, including formalgeo-structure774k [41] and SynthGeo228k [41], and is designed solely for parsing geometric diagrams into ConsCDL and ImgCDL. In contrast, our proposed MLLM Interpreter can process both diagrams and text with a unified model, while requiring only 5.5k training samples.

Comparison. Consistent with CDL matching rewards in GRPO, we evaluate CDL generation performance using recall and precision scores (see Eq. (6)) for each CDL type. As shown in Table 2, our MLLM Interpreter exhibits strong overall performance on CDL generation.

4.2.2. Plane Geometry Problem Solving

Baseline. We compare the plane geometry problem solving performance of our method with both closed-source and open-source leading MLLMs. The closed-source baselines include the available state-of-the-art (SOTA) models: GPT-4o [12], Claude series, and Gemini series [6]. For open-source MLLMs, we evaluate general-purpose reasoning models such as Qwen2.5-VL 32B [1] and GLM 4.1-V-Thinking [28], as well as previous methods specifically designed for PGPS, including G-LLaVA [8], GeoUni [5], DFE-GPS [41], and GF Reasoner [35].

Comparison. We perform open-ended evaluation and re-

Table 4. **Comparison of Plane Geometry Problem Solving performance with closed-source and open-source MLLMs.** On both in-domain and out-of-domain benchmarks, our proposed method significantly outperforms all open-source MLLMs and shows comparable performance to SOTA closed-source MLLMs.

Models	Data	Formalgeo	Unigeo	MathV.	
Closed-Source MLLMs					
GPT-4o		58.0	43.9	47.1	
Claude-Sonnet-4		69.1	72.6	60.7	
Claude-Opus-4.1		69.1	74.2	63.1	
Gemini2.5-Flash	-	80.5	82.8	79.4	
Gemini2.5-Pro		81.8	84.6	81.3	
Open-Source MLLMs					
G-LLaVA [8]	170k	-	-	56.7	
Qwen2.5-VL 32B [1]	-	57.3	67.9	66.8	
GLM4.1-V [28]	-	73.4	79.2	80.4	
GeoUni [5]	235k	59.8	-	-	
DFE-GPS [41]	238k	75.3	-	-	
GF Reasoner [35]	184k	-	72.7	64.9	
In Domain		OOD			
Ours	5.5k	85.7	84.0	80.8	

port the solving accuracy across benchmarks. As shown in Table 4, our method consistently achieves superior performance on both in-domain and out-of-domain benchmarks. With only 5.5k training data, it significantly outperforms all open-source MLLMs and attains comparable performance to state-of-the-art closed-source model Gemini2.5-Pro. Notably, on Formalgeo-Rec-CoT, we surpass Gemini2.5-Pro by 3.9% accuracy.

4.3. Ablation Study

In this section, all ablation experiments are performed with Qwen2.5-VL 7B as the MLLM Interpreter.

Concise descriptions benefit MLLM’s learning by narrowing the search space. To empirically validate that the conciseness of CDL benefits the MLLM Interpreter’s training, we conduct an ablation study (Table 5). We intentionally introduce redundant information into the ConsCDL annotations (Line 1), *e.g.*, replacing preset terms like “Shape” with more specific but unnecessary ones such as “Triangle” and “Circle Segment”. This intentional expansion of the description search space leads to a degradation in ConsCDL

Table 5. **Concise descriptions benefit MLLM Interpreter’s training by narrowing search space.** We conduct an ablation to validate that the conciseness of CDL benefits the learning of the MLLM Interpreter (Qwen2.5-VL 7B) on Formalgeo-Rec-CoT.

Concise	TextCDL		ImgCDL		ConsCDL		Acc.
	Re.	Pre.	Re.	Pre.	Re.	Pre.	
	99.1	99.1	97.0	97.0	91.6	90.7	80.5
✓	99.1	99.1	97.0	96.9	92.7	92.1	83.2

Table 6. **CDL Matching Rewards outperform the Solution-based Reward.** We train the MLLM Interpreter (Qwen2.5-VL 7B) with an extra solution-based reward provided by LLM Solver (Qwen3 30B) and observe that the sparse reward degrades the performance on Formalgeo-Rec-CoT.

Ours	Solution Reward	TextCDL		ImgCDL		ConsCDL		Acc.
		Re.	Pre.	Re.	Pre.	Re.	Pre.	
✓		99.1	99.1	97.0	96.9	92.7	92.1	83.2
✓	✓	98.9	99.0	96.4	96.5	91.5	91.1	81.3

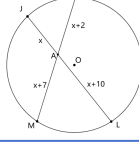
generation performance. Consequently, compared to generating the original, concise CDL (Line 2), the expanded version results in lower solving accuracy on Formalgeo7k-Rec-CoT, thereby directly confirming the benefit of a narrowed search space.

CDL Matching Rewards outperform Solution-based Reward. Table 6 compares our designed CDL matching rewards to conventional solution-based reward in GRPO. Combining solution-based reward with ours, the performance drops obviously. With solution-based reward only, there is no performance gain compared with SFT. All those results verify that CDL matching rewards are more effective than solution-based reward.

Effect of CoT in CDL generation. During the SFT stage, we augment the training data solely with ConsCDL CoT, excluding CoTs for ImgCDL and TextCDL. As evidenced by Table 3, training without CoT (row 1) severely degrades CDL quality (especially ConsCDL) and yields low solving accuracy. Introducing ConsCDL CoT (row 2) yields consistent performance improvements. However, incorporating CoTs for ImgCDL and TextCDL leads to a slight degradation. We hypothesize that generating ImgCDL and TextCDL relies more on direct perception from the diagram or caption, requiring less step-by-step reasoning than ConsCDL. Consequently, the additional CoT tokens may act as a distraction, which increases the training complexity without benefit. Considering both efficiency and performance, we only incorporate CoT of ConsCDL into training data.

Table 7. **Effect of rewards in RL stage.** In order to validate the effect of rewards in the RL stage, we perform the ablations with Qwen2.5-VL 7B on Formalgeo-Rec-CoT. Results further validate that each proposed reward contributes to a better performance.

Rewards				TextCDL		ImgCDL		ConsCDL		Formalgeo
S_C	S_I	S_T	S_f	Recall	Precision	Recall	Precision	Recall	Precision	
✓				95.9	95.8	95.7	94.1	92.0	91.8	81.0
✓	✓			96.5	96.5	97.1	97.1	92.5	91.7	82.2
✓	✓	✓		98.3	98.3	97.0	97.0	92.0	91.5	81.6
✓	✓	✓	✓	99.1	99.1	97.0	96.9	92.7	92.1	83.2



Prompt: The Caption of this geometric diagram is: As shown in the diagram, $AJ=x$, $AK=x+2$, $AM=x+7$, $LA=x+10$, the center of $\odot O$ is O. Find the value of x. Please provide the consCDL and imgCDL based on this given geometric diagram and provide the textCDL based on its caption. You first think within <think></think> tags and then provide all CDLs within <CDL></CDL> tags.

MLLM Interpreter: <think> Firstly, looking into the diagram, I see 6 points, they are L, O, J, M, A, K. And I see 1 circle, the centroid of it is O. Points JMLK lie on Circle O, they are cocircular points, so we get Cocircular(O, JMLK). Among all points, I observe their connection relationship. I see Point J and Point M are connected by Arc JM on Circle O. I see Point K and Point A are connected by line segment AJ. I see Point K and Point A are connected by line segment AK. I see Point L and Point K are connected by Arc LK on Circle O. I see Point M and Point A are connected by line segment AM. I see Point M and Point L are connected by Arc ML on Circle O. I see Point L and Point A are connected by line segment AL. I see Point K and Point J are connected by Arc KJ on Circle O. Furthermore, I observe some collinear relationship. Points J, A, L lie on a single straight line, so they are collinear and we get Collinear(JAL). Points K, A, M lie on a single straight line, so they are collinear and we get Collinear(KAM). I then look into the shapes in this geometric diagram. Now I identify some closed shapes. I identify a closed shape formed by arc KJ on circle O, line segment JA, line segment AK, represented as Shape(OKJJA,AK). I identify a closed shape formed by arc JM on circle O, line segment MA, line segment AJ, represented as Shape(OJM,MA,AJ). I identify a closed shape formed by arc LK on circle O, line segment LA, line segment AM, represented as Shape(OLM,LA,AM). I identify a closed shape formed by arc MK on circle O, line segment KA, line segment AL, represented as Shape(OLK,KA,AL). </think> <CDL> consCDL:[Shape(OKJJA,AK), Shape(OJM,MA,AJ), Shape(OLM,LA,AM), Shape(OLK,KA,AL)], 'Collinear(JAL)', 'Collinear(KAM)', 'Cocircular(O,JMLK)'], imgCDL:[Equal(LengthOfLine(AJ),x), Equal(LengthOfLine(AK),x+2), Equal(LengthOfLine(AM),x+7), Equal(LengthOfLine(LA),x+10)], textCDL:[Equal(LengthOfLine(AJ),x), Equal(LengthOfLine(AK),x+2), Equal(LengthOfLine(AM),x+7), Equal(LengthOfLine(LA),x+10)], 'IsCentreOfCircle(O,O)']. </CDL>

Reward Score

ConsCDL Score = 1.0
ImgCDL Score = 1.0
TextCDL Score = 1.0
Format Score = 1.0

GT Answer: 14

Prompt: The CDL is: consCDL:[Shape(OKJJA,AK), Shape(OJM,MA,AJ), Shape(OLM,LA,AM), Shape(OLK,KA,AL)], 'Collinear(JAL)', 'Collinear(KAM)', 'Cocircular(O,JMLK)'], imgCDL:[Equal(LengthOfLine(AJ),x), Equal(LengthOfLine(AK),x+2), Equal(LengthOfLine(AM),x+7), Equal(LengthOfLine(LA),x+10)], textCDL:[Equal(LengthOfLine(AJ),x), Equal(LengthOfLine(AK),x+2), Equal(LengthOfLine(AM),x+7), Equal(LengthOfLine(LA),x+10)], 'IsCentreOfCircle(O,O)']. The question is: Find the value of x. The final answer MUST BE put in \boxed{\{14\}}.

LLM Solver: Step 1: Identify the Chords and Their Segments. From the CDL, we are told: (1) Points J,A,L are collinear (i.e., lie on a straight line). (2) Points K,A,M are also collinear. (3) Therefore, lines JL and KM intersect at point A. (4) The points J,M,L,K lie on a circle (as Cocircular(O,JMLK)), so the intersecting chords theorem applies. We are given the following segment lengths in terms of x: (1) $AJ=x$ (2) $AL=x+10$ (3) $AK=x+2$ (4) $AM=x+7$. Step 2: Apply the Intersecting Chords Theorem. (1) According to the theorem: $AJ \cdot AL = AK \cdot AM$. (2) Substitute the known expressions: $x(x+10) = (x+2)(x+7)$. (3) Now expand both sides and set them equal, solve for x: $x=14$. Step 3: Verify the Solution. (1) Plug $x=14$ back into the original expressions: $AJ=14$, $AL=14+10=24$, $AK=14+2=16$, $AM=14+7=21$. (2) Check the products: $AJ \cdot AL = 14 \cdot 24 = 336$, $AK \cdot AM = 16 \cdot 21 = 336$. (3) Both sides match, confirming the solution is correct.

Final Answer: \boxed{14}.

Figure 3. **Qualitative Results on Formalgeo7k-Rec-CoT.** We present an example illustrating the complete pipeline of CDL Solver: an MLLM Interpreter converts geometric inputs into CDL upon which the LLM Solver performs reasoning and derives the final answer.

Effect of various RL rewards: S_f , S_C , S_I and S_T . During the RL stage, we specifically design rewards, including Format Reward S_f , ConsCDL Reward S_C , ImgCDL Reward S_I , and TextCDL Reward S_T . In order to validate the effect of each reward, we design ablations in Table 7. Results show that each reward contributes to the CDL generation and geometric problem solving performance.

4.4. Qualitative Results

We present an example on the validation set of Formalgeo7k-Rec-CoT to illustrate the complete pipeline of our proposed CDL Solver: the MLLM Interpreter converts the diagrams and captions into CDL upon which the LLM Solver performs reasoning and derives the final answer. More qualitative results can be found in the appendix.

5. Conclusion

In this paper, we observe that LLM itself is potentially a powerful PGP solver when converting visual diagram into textual descriptions. Thus, we propose a new paradigm to unleash LLM’s potential for Plane Geometry Problem Solving (PGPS). We train an MLLM Interpreter to convert geometric diagram into a concise geometric description (CDL) and then an off-the-shelf LLM Solver is utilized to perform reasoning. We design a two-stage pipeline for the training of MLLM Interpreter, including an SFT Stage with CoT-augmented data and a GRPO Stage with specifically designed CDL matching rewards. Extensive experiments demonstrate that our method achieves superior performance in both CDL generation and solving accuracy on PGP benchmarks. We hope that our work may inspire future research to investigate how to better exploit the inherent reasoning capability of LLM for complex multimodal reasoning tasks.

8

References

[1] Shuai Bai, Kebin Chen, Xuejing Liu, Jialin Wang, Wenbin Ge, Sibo Song, Kai Dang, Peng Wang, Shijie Wang, Jun Tang, et al. Qwen2.5-vl technical report. *arXiv preprint arXiv:2502.13923*, 2025. 1, 3, 5, 6, 7

[2] Tom Brown, Benjamin Mann, Nick Ryder, Melanie Subbiah, Jared D Kaplan, Prafulla Dhariwal, Arvind Neelakantan, Pranav Shyam, Girish Sastry, Amanda Askell, et al. Language models are few-shot learners. *Advances in neural information processing systems*, 33:1877–1901, 2020. 3

[3] Jiaqi Chen, Jianheng Tang, Jinghui Qin, Xiaodan Liang, Lingbo Liu, Eric Xing, and Liang Lin. Geoqa: A geometric question answering benchmark towards multimodal numerical reasoning. In *Findings of the Association for Computational Linguistics: ACL-IJCNLP 2021*, pages 513–523, 2021. 3

[4] Jiaqi Chen, Tong Li, Jinghui Qin, Pan Lu, Liang Lin, Chongyu Chen, and Xiaodan Liang. Unigeo: Unifying geometry logical reasoning via reformulating mathematical expression. In *Proceedings of the 2022 Conference on Empirical Methods in Natural Language Processing*, pages 3313–3323, 2022. 1, 2, 5

[5] Jo-Ku Cheng, Zeren Zhang, Ran Chen, Jingyang Deng, Ziran Qin, and Jinwen Ma. Geouni: A unified model for generating geometry diagrams, problems and problem solutions. *arXiv preprint arXiv:2504.10146*, 2025. 3, 6, 7

[6] Gheorghe Comanici, Eric Bieber, Mike Schaeckermann, Ice Pasupat, Noveen Sachdeva, Inderjit Dhillon, Marcel Blissein, Ori Ram, Dan Zhang, Evan Rosen, et al. Gemini 2.5: Pushing the frontier with advanced reasoning, multimodality, long context, and next generation agentic capabilities. *arXiv preprint arXiv:2507.06261*, 2025. 3, 6

[7] Daocheng Fu, Zijun Chen, Renqiu Xia, Qi Liu, Yuan Feng, Hongbin Zhou, Renrui Zhang, Shiyang Feng, Peng Gao, Junchi Yan, et al. Trustgeogen: Scalable and formal-verified data engine for trustworthy multi-modal geometric problem solving. *arXiv preprint arXiv:2504.15780*, 2025. 3

[8] Jiahui Gao, Renjie Pi, Jipeng Zhang, Jiacheng Ye, Wanjuan Zhong, Yufei Wang, Lanqing HONG, Jianhua Han, Hang Xu, Zhenguo Li, et al. G-llava: Solving geometric problem with multi-modal large language model. In *The Thirteenth International Conference on Learning Representations*. 1, 3, 6, 7

[9] Daya Guo, Dejian Yang, Haowei Zhang, Junxiao Song, Ruoyu Zhang, Runxin Xu, Qihao Zhu, Shirong Ma, Peiyi Wang, Xiao Bi, et al. Deepseek-r1: Incentivizing reasoning capability in llms via reinforcement learning. *arXiv preprint arXiv:2501.12948*, 2025. 3

[10] Zixian Guo, Ming Liu, Zhilong Ji, Jinfeng Bai, Lei Zhang, and Wangmeng Zuo. Decoupled visual interpretation and linguistic reasoning for math problem solving. *arXiv preprint arXiv:2505.17609*, 2025. 3

[11] Zihan Huang, Tao Wu, Wang Lin, Shengyu Zhang, Jingyuan Chen, and Fei Wu. Autogeo: Automating geometric image dataset creation for enhanced geometry understanding. *IEEE Transactions on Multimedia*, 2025. 3

[12] Aaron Hurst, Adam Lerer, Adam P Goucher, Adam Perelman, Aditya Ramesh, Aidan Clark, AJ Ostrow, Akila Welihinda, Alan Hayes, Alec Radford, et al. Gpt-4o system card. *arXiv preprint arXiv:2410.21276*, 2024. 3, 6

[13] Albert Q Jiang, Alexandre Sablayrolles, Antoine Roux, Arthur Mensch, Blanche Savary, Chris Bamford, Devenendra Singh Chaplot, Diego de las Casas, Emma Bou Hanna, Florian Bressand, et al. Mixtral of experts. *arXiv preprint arXiv:2401.04088*, 2024. 3

[14] Alexander Kirillov, Eric Mintun, Nikhila Ravi, Hanzi Mao, Chloe Rolland, Laura Gustafson, Tete Xiao, Spencer Whitehead, Alexander C Berg, Wan-Yen Lo, et al. Segment anything. In *Proceedings of the IEEE/CVF international conference on computer vision*, pages 4015–4026, 2023. 3

[15] Junnan Li, Dongxu Li, Caiming Xiong, and Steven Hoi. Blip: Bootstrapping language-image pre-training for unified vision-language understanding and generation. In *International conference on machine learning*, pages 12888–12900. PMLR, 2022. 3, 5

[16] Zhihao Li, Yao Du, Yang Liu, Yan Zhang, Yufang Liu, Mengdi Zhang, and Xunliang Cai. Eagle: Elevating geometric reasoning through llm-empowered visual instruction tuning. *arXiv preprint arXiv:2408.11397*, 2024. 3

[17] Haotian Liu, Chunyuan Li, Qingyang Wu, and Yong Jae Lee. Visual instruction tuning. *Advances in neural information processing systems*, 36:34892–34916, 2023. 1, 3

[18] Pan Lu, Hritik Bansal, Tony Xia, Jiacheng Liu, Chunyuan Li, Hannaneh Hajishirzi, Hao Cheng, Kai-Wei Chang, Michel Galley, and Jianfeng Gao. Mathvista: Evaluating mathematical reasoning of foundation models in visual contexts. In *The Twelfth International Conference on Learning Representations*. 2, 5

[19] OpenAI. Chatgpt, 2023. 3

[20] OpenAI. Gpt5, 2025. 3

[21] Yicheng Pan, Zhenrong Zhang, Pengfei Hu, Jiefeng Ma, Jun Du, Jianshu Zhang, Quan Liu, Jianqing Gao, and Feng Ma. Enhancing the geometric problem-solving ability of multimodal llms via symbolic-neural integration. *arXiv preprint arXiv:2504.12773*, 2025. 1

[22] Bowen Ping, Minnan Luo, Zhuohang Dang, Chenxi Wang, and Chengyou Jia. Autogps: Automated geometry problem solving via multimodal formalization and deductive reasoning. *arXiv preprint arXiv:2505.23381*, 2025. 1

[23] Alec Radford, Jong Wook Kim, Chris Hallacy, Aditya Ramesh, Gabriel Goh, Sandhini Agarwal, Girish Sastry, Amanda Askell, Pamela Mishkin, Jack Clark, et al. Learning transferable visual models from natural language supervision. In *International conference on machine learning*, pages 8748–8763. PMLR, 2021. 3

[24] Rafael Rafailov, Archit Sharma, Eric Mitchell, Christopher D Manning, Stefano Ermon, and Chelsea Finn. Direct preference optimization: Your language model is secretly a reward model. *Advances in neural information processing systems*, 36:53728–53741, 2023. 3

[25] Colin Raffel, Noam Shazeer, Adam Roberts, Katherine Lee, Sharan Narang, Michael Matena, Yanqi Zhou, Wei Li, and Peter J Liu. Exploring the limits of transfer learning with a

unified text-to-text transformer. *Journal of machine learning research*, 21(140):1–67, 2020. 5

[26] John Schulman, Filip Wolski, Prafulla Dhariwal, Alec Radford, and Oleg Klimov. Proximal policy optimization algorithms. *arXiv preprint arXiv:1707.06347*, 2017. 3

[27] Zhihong Shao, Peiyi Wang, Qihao Zhu, Runxin Xu, Junxiao Song, Xiao Bi, Haowei Zhang, Mingchuan Zhang, YK Li, Yang Wu, et al. Deepseekmath: Pushing the limits of mathematical reasoning in open language models. *arXiv preprint arXiv:2402.03300*, 2024. 2, 3, 4

[28] V Team, Wenyi Hong, Wenmeng Yu, Xiaotao Gu, Guo Wang, Guobing Gan, Haomiao Tang, Jiale Cheng, Ji Qi, Junhui Ji, Lihang Pan, Shuaqi Duan, Weihan Wang, Yan Wang, Yean Cheng, Zehai He, Zhe Su, Zhen Yang, Ziyang Pan, Aohan Zeng, Baoxu Wang, Bin Chen, Boyan Shi, Changyu Pang, Chenhui Zhang, Da Yin, Fan Yang, Guoqing Chen, Jiazheng Xu, Jiale Zhu, Jiali Chen, Jing Chen, Jin-hao Chen, Jinghao Lin, Jinjiang Wang, Junjie Chen, Leqi Lei, Letian Gong, Leyi Pan, Mingdao Liu, Mingde Xu, Mingzhi Zhang, Qinkai Zheng, Sheng Yang, Shi Zhong, Shiyu Huang, Shuyuan Zhao, Siyan Xue, Shangqin Tu, Shengbiao Meng, Tianshu Zhang, Tianwei Luo, Tianxiang Hao, Tianyu Tong, Wenkai Li, Wei Jia, Xiao Liu, Xiaohan Zhang, Xin Lyu, Xinyue Fan, Xuancheng Huang, Yanling Wang, Yadong Xue, Yanfeng Wang, Yanzi Wang, Yifan An, Yifan Du, Yiming Shi, Yiheng Huang, Yilin Niu, Yuan Wang, Yuanchang Yue, Yuchen Li, Yutao Zhang, Yuting Wang, Yu Wang, Yuxuan Zhang, Zhao Xue, Zhenyu Hou, Zhengxiao Du, Zihan Wang, Peng Zhang, Debing Liu, Bin Xu, Juanzi Li, Minlie Huang, Yuxiao Dong, and Jie Tang. Glm-4.5v and glm-4.1v-thinking: Towards versatile multimodal reasoning with scalable reinforcement learning, 2025. 1, 3, 6, 7

[29] Hugo Touvron, Thibaut Lavril, Gautier Izacard, Xavier Martinet, Marie-Anne Lachaux, Timothée Lacroix, Baptiste Rozière, Naman Goyal, Eric Hambro, Faisal Azhar, et al. Llama: Open and efficient foundation language models. *arXiv preprint arXiv:2302.13971*, 2023. 3

[30] Hugo Touvron, Louis Martin, Kevin Stone, Peter Albert, Amjad Almahairi, Yasmine Babaei, Nikolay Bashlykov, Soumya Batra, Prajjwal Bhargava, Shruti Bhosale, et al. Llama 2: Open foundation and fine-tuned chat models. *arXiv preprint arXiv:2307.09288*, 2023. 3

[31] Haoran Wei, Youyang Yin, Yumeng Li, Jia Wang, Liang Zhao, Jianjian Sun, Zheng Ge, Xiangyu Zhang, and Daxin Jiang. Slow perception: Let’s perceive geometric figures step-by-step. *arXiv preprint arXiv:2412.20631*, 2024. 3

[32] Liangyu Xu, Yingxiu Zhao, Jingyun Wang, Yingyao Wang, Bu Pi, Chen Wang, Mingliang Zhang, Jihao Gu, Xiang Li, Xiaoyong Zhu, et al. Geosense: Evaluating identification and application of geometric principles in multimodal reasoning. *arXiv preprint arXiv:2504.12597*, 2025. 3

[33] Cilin Yan, Jingyun Wang, Lin Zhang, Ruihui Zhao, Xiaopu Wu, Kai Xiong, Qingsong Liu, Guoliang Kang, and Yangyang Kang. Efficient and accurate prompt optimization: the benefit of memory in exemplar-guided reflection. In *Proceedings of the 63rd Annual Meeting of the Association for Computational Linguistics (Volume 1: Long Papers)*, pages 753–779, Vienna, Austria, 2025. Association for Computational Linguistics. 3

[34] An Yang, Anfeng Li, Baosong Yang, Beichen Zhang, Binyuan Hui, Bo Zheng, Bowen Yu, Chang Gao, Chengen Huang, Chenxu Lv, et al. Qwen3 technical report. *arXiv preprint arXiv:2505.09388*, 2025. 3, 5

[35] Tianyun Yang, Yunwen Li, Ziniu Li, Zhihang Lin, Ruoyu Sun, and Tian Ding. Bridging formal language with chain-of-thought reasoning to geometry problem solving. *arXiv preprint arXiv:2508.09099*, 2025. 3, 6, 7

[36] Qiyi Yu, Zheng Zhang, Ruofei Zhu, Yufeng Yuan, Xiaochen Zuo, Yu Yue, Weinan Dai, Tiantian Fan, Gaohong Liu, Lingjun Liu, et al. Dapo: An open-source llm reinforcement learning system at scale. *arXiv preprint arXiv:2503.14476*, 2025. 3

[37] Hao Zhang, Feng Li, Shilong Liu, Lei Zhang, Hang Su, Jun Zhu, Lionel Ni, and Heung-Yeung Shum. Dino: Detr with improved denoising anchor boxes for end-to-end object detection. In *The Eleventh International Conference on Learning Representations*, . 3

[38] Ming-Liang Zhang, Fei Yin, and Cheng-Lin Liu. A multi-modal neural geometric solver with textual clauses parsed from diagram. In *Proceedings of the Thirty-Second International Joint Conference on Artificial Intelligence*, pages 3374–3382, 2023. 1, 3

[39] Renrui Zhang, Xinyu Wei, Dongzhi Jiang, Ziyu Guo, Yichi Zhang, Chengzhuo Tong, Jiaming Liu, Aojun Zhou, Shanghang Zhang, Peng Gao, et al. Mavis: Mathematical visual instruction tuning with an automatic data engine. In *The Thirteenth International Conference on Learning Representations*, . 3

[40] Xiaokai Zhang, Na Zhu, Yiming He, Jia Zou, Qike Huang, Xiaoxiao Jin, Yanjun Guo, Chenyang Mao, Yang Li, Zhe Zhu, et al. Formalgeo: An extensible formalized framework for olympiad geometric problem solving. *arXiv preprint arXiv:2310.18021*, 2023. 2, 3

[41] Zeren Zhang, Jo-Ku Cheng, Jingyang Deng, Lu Tian, Jinwen Ma, Ziran Qin, Xiaokai Zhang, Na Zhu, and Tuo Leng. Diagram formalization enhanced multi-modal geometry problem solver. In *ICASSP 2025-2025 IEEE International Conference on Acoustics, Speech and Signal Processing (ICASSP)*, pages 1–5. IEEE, 2025. 1, 5, 6, 7, 2

[42] Na Zhu, Xiaokai Zhang, Qike Huang, Fangzhen Zhu, Zhenbing Zeng, and Tuo Leng. Fgeo-parser: Autoformalization and solution of plane geometric problems. *Symmetry*, 17(1):8, 2024. 1, 2, 3, 5, 6

Concise Geometric Description as a Bridge: Unleashing the Potential of LLM for Plane Geometry Problem Solving

Supplementary Material

Table 8. **Effect of rollout number N in the GRPO stage.** We perform the experiments on Qwen2.5-VL 7B. Accounting for both training cost and performance, we set $N = 8$.

Performance		$N = 5$	$N = 8$	$N = 10$
TextCDL	Recall	98.5	99.1	98.3
	Precision	98.4	99.1	98.3
ImgCDL	Recall	96.9	97.0	97.0
	Precision	96.9	96.9	97.0
ConsCDL	Recall	89.1	92.7	91.0
	Precision	87.9	92.1	90.3
Formalgeo-Rec-CoT		80.9	83.2	82.5

Table 9. **Effect of Reward Weights α, γ in GRPO.** We perform the experiments on Qwen3-VL 8B. According to results, we set $\alpha = 0.1, \gamma = 0.5$.

α	γ	TextCDL		ImgCDL		ConsCDL		Acc.
		Re.	Pre.	Re.	Pre.	Re.	Pre.	
0.2	0.4	98.3	98.9	96.8	96.8	96.1	96.0	84.4
0.4	0.3	98.4	99.0	97.2	97.0	96.1	96.0	83.6
0.1	0.5	99.2	99.3	97.0	96.9	95.9	95.8	85.7

6. More Ablations

Effect of rollout number N in GRPO. In order to validate the effect of rollout number N in the GRPO stage, we perform an ablation study on Qwen2.5-VL 7B in Table 8. Setting $N = 10$ yields no performance gain on CDL generation and slightly degrades the problem solving accuracy. Moreover, it brings an extra 80 hours of training time compared with $N = 8$. Considering the training cost and the performance, we set $N = 8$.

Effect of Reward Weights α, γ in GRPO. In order to validate the effect of reward weights α, γ in the GRPO stage, we perform an ablation study on Qwen3-VL 8B in Table 9. Considering the CDL generation performance and the solving accuracy, we set $\alpha = 0.1, \gamma = 0.5$.

Superior Performance on Original Formalgeo7k v2. In Table 10, we conduct both training and evaluation on the

Table 10. **Superior Performance on Original Formalgeo7k v2.** We further conduct both training and evaluation on the original Formalgeo7k v2. Compared with previous methods, our superior performance on the original Formalgeo7k v2 validates the effectiveness of our framework.

Methods	TextCDL		ImgCDL		ConsCDL	
	Re.	Pre.	Re.	Pre.	Re.	Pre.
FgeoParser (Diag.)	-	-	77.5	-	87.0	-
FgeoParser (Text)	96.5	-	-	-	-	-
Diagram Formalizer	-	-	92.9	-	90.3	-
Ours (Formalgeo7k)	98.2	98.3	97.0	97.0	91.0	90.3
Ours (Rec-CoT)	99.1	99.1	97.0	96.9	92.7	92.1

original Formalgeo7k v2 (“Ours (Formalgeo7k)” in the table). The results demonstrate that our method outperforms previous CDL generation approaches even when using the original data, validating the effectiveness of our framework. Furthermore, training with the refined data yields better performance, confirming that high-quality CDL annotations are also beneficial.

Empirical analysis of how concise descriptions benefit MLLM’s learning. We further compare the performance of concise CDL against the expanded version on the Formalgeo-Rec-CoT training set. While results in Table 11 show that the expanded version achieves slightly higher CDL matching scores on the training set, its performance on the validation set is inferior to our concise CDL (as shown in Table 5). This phenomenon shows the relatively poor generalization of the expanded version compared to ours. The expanded version introduces unnecessary or redundant information, which unexpectedly enlarges the search space. Consequently, with relatively limited samples, MLLM tends to memorize training samples rather than learning generalizable patterns. In contrast, the search space of concise CDL is smaller, which eases the generalization.

Generalization of CDL for various LLM Solvers. In order to validate the generalization capability of our proposed diagram, we further perform an ablation for various LLM Solvers. Taking the generated CDL from our MLLM Interpreter (Qwen2.5-VL 7B) as inputs, we uti-

Table 11. **Concise descriptions (ours) v.s. Expanded version on the training set.** While the expanded version achieves slightly higher scores than the concise CDL on the training set, its performance on the validation set (shown in Table 5) degrades, which shows poor generalization.

Type	TextCDL		ImgCDL		ConsCDL	
	Re.	Pre.	Re.	Pre.	Re.	Pre.
Concise	99.3	99.4	98.7	98.5	93.8	94.1
Expanded	99.8	99.8	98.7	98.7	94.0	94.1

lize various LLMs to serve as solvers, including Qwen3 30B, Qwen3 32B, DeepSeek-V3.1-Terminus, and GLM-4.6. Results in Table 12 demonstrate that our proposed paradigm achieves overall superior performance against previous methods across LLM solvers, validating its strong generalization. Qwen3 30B yields the best result and is therefore selected as the LLM solver in our main paper.

Solving Accuracy Comparison with Diagram Formalizer on the same LLM Solver. We further evaluate end-to-end solving accuracy improvements against DFE-GPS’s Diagram Formalizer [41] across both in-domain (Formalgeo7k v2) and Out-Of-Domain (Unigeo & Mathvista) benchmarks. CDL generation results of Diagram Formalizer are obtained by running its official code. In Table 13, using the **same LLM solver (Qwen3 30B)**, ours yields consistent improvement across all benchmarks, further validating our generalization capability and confirming that enhancement on CDL generation indeed leads to better solving performance.

7. Proof for CDL’s Conciseness

In this section, we provide a proof to demonstrate the conciseness of Conditional Declaration Language (CDL) compared with general textual descriptions.

Generally, a textual description of a geometric input can be decomposed into three components: 1) shape descriptions that depict geometric shapes, *e.g.*, line segments, angles, triangles, *etc.*, 2) relation descriptions that reflect the positional and algebraic relationships between shape elements, and quantitative metric (*e.g.*, the line segment length and the angle degree), and 3) irrelevant words that are irrelevant to any geometric shapes or relations, *e.g.*, “a”, “the”, *etc.*

For a specific geometric input, let H , R , and O denote the sets of all possible shapes, relations, and irrelevant words, respectively, under specific constraints or rules (*e.g.*, CDL rules).

(1) **Shape Descriptions:** In CDL, the shape description set H^C consists of closed shapes, angles, and line segments.

Table 12. **Generalization of CDL for various LLM Solvers.** We perform experiments with various LLM Solvers on Formalgeo-Rec-CoT. All LLM Solvers take the generated CDL from our MLLM Interpreter (Qwen2.5-VL 7B) as inputs to perform reasoning.

	Models	Formalgeo
Closed-Source MLLMs		
	GPT-4o	58.0
	Claude-Sonnet-4	69.1
	Claude-Opus-4.1	69.1
	Gemini2.5-Flash	80.5
	Gemini2.5-Pro	81.8
Open-Source MLLMs		
	Qwen2.5-VL 32B	57.3
	Qwen3-VL 30B	80.1
	GLM4.1-V	73.4
	GeoUni	59.8
	DFE-GPS	75.3
Ours		
MLLM Interpreter	+Qwen3 32B	82.5
	+GLM-4.6	82.3
	+DeepSeek V3.1	79.4
	+Qwen3 30B	83.2

Table 13. **Solving Accuracy Comparison with Diagram Formalizer on the same LLM Solver.** We evaluate end-to-end solving accuracy improvements against DFE-GPS’s Diagram Formalizer on the same LLM Solver, Qwen3 30B. Results demonstrate the generalization capability of our method and confirm that enhancement on CDL generation indeed leads to better solving performance.

Models	LLM	Formalgeo	Unigeo	MathV.
DFE-GPS	Qwen3	80.3	79.9	69.0
Ours	Qwen3	85.7	84.0	80.8

There are two constraints: a) the closed shape cannot be decomposed further into other closed shapes; b) the angle does not exist in any closed shape in the diagram; the line segment does not exist in any angle or closed shape in the diagram. While in general textual descriptions H^T , there

is no such constraint. Thus, in H^T , in addition to elements in H^C , there may also exist closed shapes that can be decomposed further and angles or line segments that exist in a specific closed shape. Consequently, $H^C \subseteq H^T$ and $|H^C| \leq |H^T|$.

(2) **Relation Descriptions:** Suppose we need to depict K relations to solve our problem. For each piece of relation, there is only one possible description for such a relation in CDL. So in total, $|R^C|$ of CDL equals the number of relations K . However, there are many choices for describing the same relation in general textual descriptions. Thus, in total $|R^T| \gg K$.

(3) **Irrelevant Words:** As CDL is a description language with a predefined format, CDL doesn't contain any irrelevant words. Thus, the O^C for CDL and O^T for general text satisfy $|O^C| = 0 \ll |O^T|$.

Therefore, for any given geometric input, the following inequality satisfies:

$$|\text{CDL}| = |H^C| + |R^C| + |O^T| \ll |H^T| + |R^T| + |O^T| = |\text{Text}|.$$

This inequality proves that for a given geometric input, the number of all possible descriptions in CDL $|\text{CDL}|$ is much smaller than that in general textual descriptions $|\text{Text}|$, *i.e.*, the CDL description is more concise than the general textual description. We provide an illustration to demonstrate this in Fig. 4.

8. More Qualitative Results

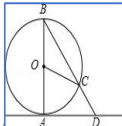
In this section, we provide examples of various benchmarks, including Formalgeo-Rec-CoT, Unigeo, and Mathvista.

Diagram	Description	General Text
	<p>ConsCDL: Shape(AB,BC,CA), Shape(AC,CD,DA) Collinear(BCD) ImgCDL: Perpendicular(AC,CD) TextCDL: Perpendicular(AC,BD)</p>	<p>The image displays a triangle labeled ABD. Triangle ABD is further divided into two triangles labeled ABC and ACD by line segment AC. Point C lies on BD. Looking into the diagram, right angle symbol is shown at point C, indicating that the line segment AC forms a 90-degree angle with the base BD. From the caption, AC is perpendicular to BD.</p>
	<p>Shape(AB,BC,CA) (basic) Shape(AB,BC,CA) Shape(BC,CA,AB) Shape(CA,AB,CB)</p>	<p>Triangle ABD (composition) $\triangle ABD \triangle ADB$ $\triangle BDA \triangle BAD$ $\triangle DAB \triangle DBA$</p>
	<p>Shape(AC,CD,DA) (basic) Shape(AC,CD,DA) Shape(CD,DA,AC) Shape(DA,AC,CD)</p>	<p>Triangle ABC (basic) $\triangle ABC \triangle ACB$ $\triangle BCA \triangle BCD$ $\triangle CAB \triangle CDA$</p>

Figure 4. **Illustration of CDL’s Conciseness.** A textual description of a geometric diagram can be decomposed into **shape descriptions (H)**, **relation descriptions (R)**, and **irrelevant words (O)**. We use “basic” to denote the triangles that cannot be decomposed further, and “composition” to denote the complex triangles composed of two basics. Under specific constraints in the CDL rule, $|H^C|$, $|R^C|$, and $|O^C|$ are minimal to $|H^T|$, $|R^T|$, and $|O^T|$, respectively. Therefore, for any given geometric diagram, a CDL description is significantly more concise than a general textual description.

Figure 5. Qualitative Result on Formalgeo7k-Rec-CoT.

Figure 6. Qualitative Result on Unigeo



GT Answer: 50

Prompt: The Caption of this geometric diagram is: As shown in the figure, AB is the diameter of $\odot O$, point C is on $\odot O$, AE is the tangent of $\odot O$, A is the tangent point, connect BC and extend to intersect AE at point D. If $\angle AOC = 80.0$, then the degree of $\angle ADB$ is (). Please provide the consCDL and imgCDL based on this given geometric diagram and provide the textCDL based on its caption. You first think within <think> tags and then provide all CDLs within <CDL></CDL> tags.

MLLM Interpreter: **think:** Firstly, looking into the diagram, I see 6 points, they are C, E, B, O, D, A. And I see 1 circle, the centred of it is O. Points BAC lie on Circle O, they are cocircular points, so we get Cocircular(O, BAC). Among all points, I observe their connection relationship. I see Point A and Point D are connected by line segment AD. I see Point A and Point D are connected by line segment AD. I see Point C and Point O are connected by line segment CO. I see Point A and Point D are connected by line segment AD. I see Point C and Point B are connected by line segment BC. I see Point D and Point C are connected by line segment CD. I see Point B and Point O are connected by line segment BO. I see Point O and Point A are connected by line segment AO. I see Point A and Point C are connected by Arc AC on Circle O. I see Point B and Point A are connected by Arc BA on Circle O. I see Point C and Point B are connected by Arc CB on Circle O. Furthermore, I observe some collinear relationship. Points B, O, A lie on a single straight line, so they are collinear and we get Collinear(BOA). Points B, C, D lie on a single straight line, so they are collinear and we get Collinear(BCD). Points A, D, E lie on a single straight line, so they are collinear and we get Collinear(ADE). I then look into the shapes in this geometric diagram. Now I identify some closed shapes. I identify a closed shape formed by arc BA on circle O, line segment AO, line segment OB, represented as Shape(OBA,AO,OB). I identify a closed shape formed by arc CB on circle O, line segment BC, represented as Shape(OCB,BC). I identify a closed shape formed by line segment OC, line segment CB, line segment BO, represented as Shape(OC,CB,BO). I identify a closed shape formed by arc AC on circle O, line segment AD, line segment DC, represented as Shape(OAC,AD,DC). **think:** <CDL>-consCDL-[Shape(OBA,AO,OB), 'Shape(OAC,CO,OA)', 'Shape(OC,CB,BC)', 'Shape(OC,BC,BO)', 'Shape(OAC,AD,DC)', 'Collinear(BCD)', 'Collinear(ADE)', 'Cocircular(O,BAC)', 'Shape(OC,BC,BO)', 'Shape(OAC,AD,DC)', 'Collinear(BOA)', 'Shape(OAC,AD,DC)', 'Collinear(BCD)', 'Collinear(ADE)', 'Cocircular(O,BAC)', imgCDL[], textCDL-[IsDiameterOfCircle(AB,O), IsCentreOfCircle(O,O), IsTangentOfCircle(AE,O), 'Equal(MeasureOfAngle(AOC),80.0)'] <CDL>

Prompt: The CDL is: consCDL-[Shape(OBA,AO,OB), 'Shape(OAC,CO,OA)', 'Shape(OC,CB,BC)', 'Shape(OC,BC,BO)', 'Shape(OAC,AD,DC)', 'Collinear(BCD)', 'Collinear(ADE)', 'Cocircular(O,BAC)', imgCDL[], textCDL-[IsDiameterOfCircle(AB,O), IsCentreOfCircle(O,O), IsTangentOfCircle(AE,O), 'Equal(MeasureOfAngle(AOC),80.0)']. The question is: then the degree of $\angle ADB$ is (). The final answer MUST BE put in 'boxed()'.

LLM Solver: We analyze the geometric configuration based on the given CDL. The key Geometric Facts from the CDL: 1) AB is a diameter of the circle with center O. This implies that $OA=OB=\pi$, and $\angle ACB=90$ (by Thales' Theorem). 2) AE is tangent to the circle at point A. By the Tangent-Chord Angle Theorem, the angle between the tangent AE and chord AC is equal to the angle in the alternate segment. Therefore $\angle CAE=\angle ABC$. 3) Point D lies on both line BC and line AE. So D is the intersection of the tangent line AE and the secant line BC. Step-by-Step Derivation. Step 1: Determine $\angle ABC$. Since $\angle AOC=80$, and it's a central angle over arc AC, the inscribed angle $\angle ABC=40$. Step 2: Use Tangent-Chord Angle Theorem. From the theorem, $\angle CAE=\angle ABC=40$. Also, since AE is tangent at A, and OA is perpendicular to AE, we have $\angle OAE=90$. Thus, $\angle BAE=90-40=50$. Step 3: Analyze Triangle ADB. In triangle ADB, we use the triangle angle sum. $\angle ADB=180-\angle DAB-\angle ABD=90-40=50$.

Final Answer: **boxed(50).**

Figure 7. Qualitative Result on MathVista.